

# INVESTIGATION INTO THE EFFICACY OF CO<sub>2</sub> LASERS FOR MODIFYING THE FACTORS INFLUENCING BIOCOMPATIBILITY OF A POLYMERIC BIOMATERIAL IN COMPARISON WITH AN F<sub>2</sub> EXCIMER LASER

Paper (M604)

D. G. Waugh<sup>1</sup>, J. Lawrence<sup>1</sup>, C. D. Walton<sup>2</sup> and R. B. Zakaria<sup>2</sup>

<sup>1</sup> Wolfson School of Mechanical and Manufacturing Engineering, Loughborough University, Leicestershire, LE11 3TU, UK

<sup>2</sup> Department of Physical Sciences, Physics, University of Hull, Kingston-Upon-Hull, HU6 7RX, UK

## Abstract

Enhancement of the biocompatibility of a material by means of laser radiation has been amply demonstrated previously. Due to efficient absorption of the energy, short wavelengths and energies per pulse, polymers are usually processed using UV lasers, but the processing of polymers with IR lasers has also been demonstrated previously. In this work a comparative study for the surface modification of nylon 6,6 has been conducted in order to vary the parameters driving biocompatibility (surface topography, hydrophobic reactions, hydrophilic reactions and surface chemistry) using CO<sub>2</sub> and excimer lasers. Topographical changes were analysed using white light interferometry which indicated that both laser systems could be implemented for modifying the topography of nylon 6,6. Variations in the surface chemistry were evaluated using EDX and XPS analysis and showed that the O<sub>2</sub> increased and decreased for the CO<sub>2</sub> and F<sub>2</sub> laser irradiated samples, respectively. Modification of the hydrophobic and hydrophilic reactions was quantified by measuring the contact angle, which was found to increase in all instances for both laser systems. It is proposed that the increase in contact angle, especially for the CO<sub>2</sub> laser irradiated samples, is due to a change in wetting regime as a result of the surface pattern produced.

## Introduction

It has been demonstrated previously by others that nylon can be utilized within the biomaterial industry [1] as sutures [2], vascular grafts and other hard tissue implants [3]. However, the common theme emanating from past work is that the polymer surface does not give rise to adequate cell adhesion and proliferation. As a result of this one can see that it may be an advantage to devise a technique which would allow the bioactivity of the nylon to be increased. Numerous techniques have been developed to produce surfaces that have the ability to do this. Some of these methods are radiation grafting [4], plasma surface modification [5,6] and using various coatings [7]. Laser

surface modification [8,9] is another method which has the ability to improve bioactivity and offers a number of benefits:

- Relative cleanliness.
- Accurate processing.
- Allows much control over the heat affected zone (HAZ) due to the ability of relative precise control over the thermal profile and thermal penetration/absorption.
- Precise placement of the beam onto the target material allowing user specified areas of the target material to be processed.
- Non-contact processing.

The CO<sub>2</sub> laser is one of the most used lasers throughout the scientific world and within many industries because it is one of the most versatile. It is capable of emitting radiation within the infra-red (IR) region of the electromagnetic spectrum on rotational-vibrational transitions with wavelengths ranging from 9 to 11µm [10]. Due to the versatility and high powers that these lasers can achieve they have been implemented for many years in the general field of materials processing. Specific to polymers, IR lasers give rise to resonant coupling in the form of bond and lattice vibrations allowing for the processing to be thermolytical. This is due to the fact that the photon is only weakly absorbed by the polymer, with the energy that has been absorbed being distributed to vibrational modes [11].

Ultraviolet (UV) excimer lasers have also been seen to be an extremely versatile tool. Since they offer relatively small operating wavelengths and have high energies per pulse, these lasers have also been employed for materials processing over a number of years. They also have other applications in areas such as medicine [12-14], photolithography and the

pumping of dye lasers [10]. With regards to the processing of polymers, UV lasers tend to give rise to the absorption of the light through electronic excitation which is often within delocalized electron configurations. In consequence polymers can have broad absorption features and directly break the polymer bonds as a result of the high photon energy [15]. With most lasers it is seen that the smallest possible features that can be achieved are on the micron scale; however, nano-structures have been achieved using a laser emitting at a wavelength of 157nm [16].

Previous and current research has shown that it is imperative that any biomaterial should be optimized such that it can function appropriately and efficiently within the desired biological environment. In many applications it is seen that the bulk properties of a biomaterial are decided upon such that the surface properties are compromised [17,18]. For instance, this is seen throughout the use of polymeric biomaterials as they offer excellent bulk properties for biological applications; however, they possess surface properties that do not lend themselves to high performance in regards to cell adhesion and proliferation [19]. As a result of this, one can see that it would be necessary to attempt and vary the surface properties of the material without changing the bulk properties in order to influence the wettability and biocompatibility characteristics. The role of wettability in biomaterials science has been one of the most interesting subject areas in biomaterials surface science for a number of years and has allowed many to endeavour to determine the complex links between surface wetting and bioactivity [20]. A number of theories have been put forward in order to explain this phenomenon in which they usually fall into two basic categories. The first attempts to correlate the surface energy with the biomimetic properties whilst the second involves water solvent properties near the surface in which a correlation between the contact angle and biocompatibility is strived for. It should be noted; however, that in both of these categories arises a fundamental factor in which the surface energy/wetting is related somewhat to the biological response [21]. Many researchers have taken various approaches as to ascertain quantitative reasoning to bioactivity such as Van Oss *et al.* [22] by utilizing the 'equation of state' approach to calculate interfacial tensions from previously measured contact angles in order to attempt and predict cell adhesion. Such approaches have been found to fall short for determining a quantitative theory regarding the bioactivity of a material. Through the available literature it can be seen that extensive research is now being carried out regarding this in the

attempt to link wettability and bioactivity of materials [23,24].

Both CO<sub>2</sub> and excimer lasers can be employed to produce variations in surface characteristics which can lead to a manipulation of the bioactivity of a material with regards to cell adhesion and proliferation [9,18]. In this paper, two very different laser systems are used and compared to produce surface variations in nylon 6,6 with the wettability characteristics being quantified.

## Experimental Technique

### CO<sub>2</sub> Laser System

The 10.6 $\mu$ m wavelength Synrad cw 10W CO<sub>2</sub> laser system, with a spot size of the order of 100 $\mu$ m, is housed at Loughborough University and uses a galvanometer scanner to scan the beam directly across the target material. The target material and laser system was held in a laser safety cabinet in which the ambient gas was air. An extraction system was used to remove any fumes produced during laser processing. In order to generate the required marking pattern the Synrad Winmark software version 2.1.0, build 3468 was used. In addition, the software was capable of using images saved as .dxf files which can be produced by using CAD programs such as, in this case, Licom AutoCaM

### F<sub>2</sub> Excimer Laser System

The Lambda Physik LPF 202 F<sub>2</sub> excimer laser system with a wavelength of 157nm is housed at the University of Hull and utilizes a projection etching system to irradiate the target material. The beam outputting from this laser had to be fully encased in a vacuum chamber running at pressure of around 2 $\times$ 10<sup>-3</sup> mbar. This is due to the fact that 157nm light is strongly absorbed in ambient air. A diagram of the projection etching system can be seen in Figure 1.

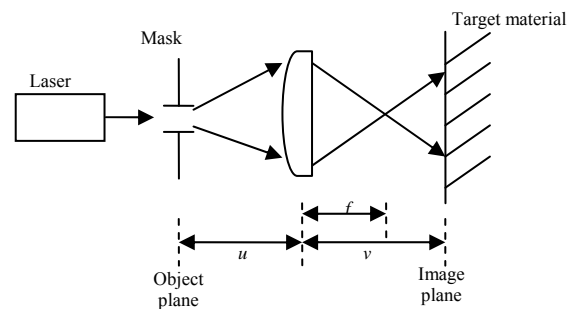


Figure 1 – Schematic diagram showing the projection etching system used

With  $u$  being the object distance,  $v$  being the image distance and  $f$  the focal length of the lens. Prior to any experimentation being carried out it was necessary to determine the required image plane.

In order to achieve the required trench dimensions an aperture projection mask was produced (Laser Micromachining, Ltd) using SS316 foil. The mask was 30mm×30mm and consisted of an array of five apertures with a diameter of 0.5mm in a straight line spaced by 1mm centre to centre. This allowed 50µm wide trenches to be etched, spaced by 50µm upon using a demagnification of 10.

### Laser Irradiation Procedures

The nylon 6,6 was sourced in 100mm×100mm sheets with a thickness of 5mm (Goodfellow Cambridge, Ltd). To obtain a conveniently sized sample for experimentation, the as-received nylon sheet was cut into 30mm diameter discs using a 1kW cw CO<sub>2</sub> laser (Everlase S48; Coherent Ltd). No discernible HAZ was observed under optical microscopic examination.

For the Synrad CO<sub>2</sub> laser system, trenches were produced with spacings of 50 and 100µm (sample C10 and C9, respectively) by scanning the beam across the target material. To produce these spacings, each experiment was carried out twice: firstly using a power of 50% (5W) with a velocity of 1000mms<sup>-1</sup> and secondly using a power of 80% (8W) with the same velocity.

The Lambda Physik LPF 202 F<sub>2</sub> excimer laser system was used to produce two areas of etched trenches by traversing the stage and keeping the beam stationary. The first of these being to achieve an etch depth of approximately 1µm (sample F3) and the second giving a depth of approximately 10µm (sample F4). In order to achieve these depths each site required 1,000 and 10,000 pulses, respectively, as the etch depth per pulse was approximately 1nm per pulse. With this in mind it was possible to determine the traverse velocities,  $v_t$ , by using Equation (1).

$$v_t = \frac{DR}{N} \quad (1)$$

Where  $D$  is the diameter of one of the apertures in the mask,  $R$  is the repetition rate (which was 20Hz) and  $N$  is the number of pulses. Upon using this equation it was determined that for 1µm and 10µm deep trenches velocities of 0.01 and 0.001mms<sup>-1</sup> were to be used, respectively.

### Mechanical Roughening Procedure

For further verification of laser induced contact angle modification two samples were roughened manually using DA-F P220 emery paper. One sample was roughened using a zig-zag motion traversing from the top to the bottom of the sample (sample R1). The second sample (sample R2) was roughened by carrying out the same technique as the first sample, with the addition of rotating the sample through 90° and repeating the roughening method with the emery paper.

### Topography, Wettability Characteristics and Surface Chemistry Analysis

After the laser irradiation of the nylon 6,6 samples they were analysed using a number of techniques. An optical microscope (Flash 200 Smartscope; OGP Ltd) was used to obtain optical micrographs of the samples. The surface profiles were determined using a white light interferometer (WLI) (NewView 500; Zygo, Ltd) with MetroPro and TalyMap Gold Software. The Zygo WLI was setup using a ×10 Mirau lens with a zoom of ×0.5 and working distance of 7.6mm. This system also allowed Sa, Ra and Wa roughness parameters to be determined for each sample.

The samples were ultrasonically cleaned in isopropanol (Fisher Scientific, Ltd) for 3 minutes at room temperature before using a sessile drop device to determine various wettability characteristics, in accordance with the procedure detailed by Rance [25]. This was to allow for a relatively clean surface prior to any contact angle measurements being taken. The sessile drop device used was a Dataphysics OCA20 with SCA20 Software. This allowed the recent advancing and receding contact angles for triply distilled water and the recent advancing angle for diodomethane to be determined for each sample. By achieving the advancing and receding contact angles the hysteresis for the system was determined. In addition, by knowing the advancing contact angles for the two liquids it was possible to use the software to draw a Owens, Wendt, Rabel and Kaeble (OWRK) plot to determine the surface energy of the samples. For the two reference liquids the SCA20 software used the Ström et al. technique to calculate the surface energy of the material. It should be noted here that 10 contact angles, using 2 droplets, in each instance was recorded to achieve a mean contact angle for each liquid and surface.

Selected samples were analysed using X-ray photoelectron spectroscopy (XPS) and were also sputter coated with Au to attain adequate conductance and analysed using scanning electron microscopy

(SEM) and energy dispersive X-ray (EDX) analysis. This allowed any surface modifications in terms of chemical composition due to the laser irradiation to be revealed.

## Results and Discussion

### Optical Microscopy Analysis

In order to effectively and completely compare the laser irradiated samples an optical micrograph of the non-irradiated material was obtained, as can be seen in Figure 2.

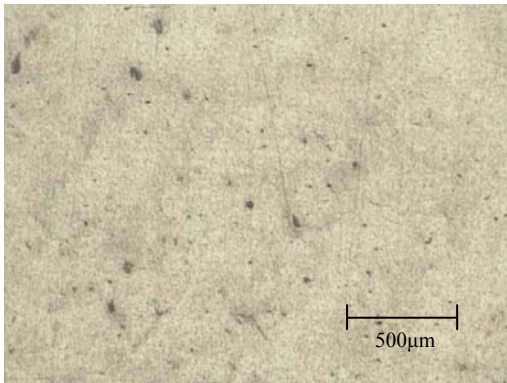


Figure 2 – Optical micrograph of the non-irradiated nylon 6,6 sample (Sample N6).

The optical micrograph of the non-irradiated sample shown in Figure 2 appears to have a minimal surface topography. The black dots on the image arise from the debris from the cutting of the samples. This debris was removed during the ultrasonic cleaning.

It was seen that both laser systems gave the ability to produce relatively good quality µm features in the nylon 6,6 samples. With regards to the trenches produced by the CO<sub>2</sub> laser, with a distance of 50µm between each trench, it can be seen in Figure 3 that no distinct trench lines had been produced.

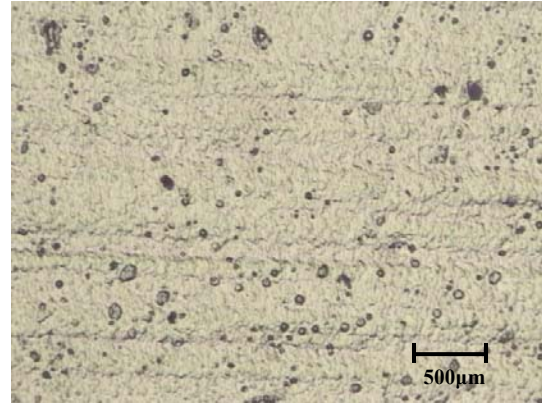


Figure 3 – Optical micrograph of nylon 6,6 CO<sub>2</sub> laser irradiated sample using 8W, 1000mm<sup>s</sup><sup>-1</sup>.

From Figure 3 it is possible to visualize that the CO<sub>2</sub> beam was scanned horizontally across the sample. However, as the spot size of the CO<sub>2</sub> laser was of the order of 100µm the scan overlapped itself so that no distinct grooves were left in the material. In addition to this, gas bubble rupture sites can be seen on the surface which is considered to be as a result of the melting and re-solidification of the nylon 6,6 following CO<sub>2</sub> laser irradiation. Also, as a consequence of the melting it appears that the material does not ablate with the CO<sub>2</sub> laser and as the material re-solidifies it produces a protrusion away from the surface. Owing to this phenomenon any trenches produced would arise due to two straight parallel protrusions, with the unirradiated part of the sample being the bottom of the trench. In comparison, the F<sub>2</sub> excimer laser produces grooves that are considerably better defined, as can be seen in Figure 4. One other major difference that the F<sub>2</sub> excimer laser offers is that the trenches are ablated and etched into the nylon 6,6 sample.

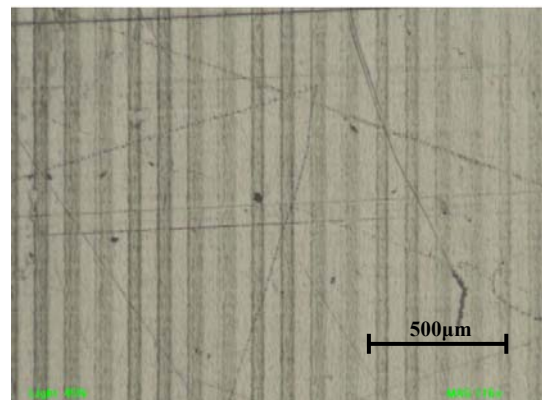


Figure 4 – Optical micrograph of trenches produced using the F<sub>2</sub> excimer laser using 1000 pulses per site, a fluence of 40mJcm<sup>2</sup> and a repetition rate of 20Hz (Sample F3).

## White Light Interferometry Analysis

The Zygo WLI and TalyMap Gold software were employed to elucidate the surface properties of the laser irradiated surfaces. Figure 5 shows the continuous axonometric with regards to the non-irradiated nylon 6,6 sample.



Figure 5 – Continuous axonometric image for the non-irradiated reference sample. (Sample N6)

Figure 5 shows how much smoother the surface of the nylon 6,6 was prior to laser irradiation, having an Sa value of only  $0.038\mu\text{m}$ . This smoothness was also confirmed by taking a profile extraction of the surface, which can be seen in Figure 6.

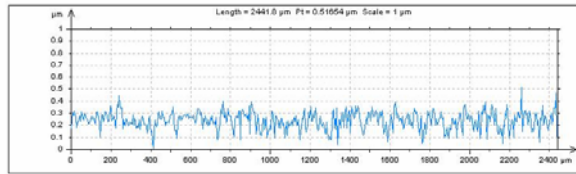


Figure 6 – Profile extraction of the surface shown in Figure 5.

The graph shown in Figure 6 allows one to see that maximum peak heights of the surface topography was approximately  $0.3\mu\text{m}$ . In comparison, the  $\text{CO}_2$  laser irradiated samples are considerably rougher than the reference sample indicating that considerable surface topography changes of nylon 6,6 are possible by this means. Figures 7 and 8 show continuous axonometric images for the  $\text{CO}_2$  laser irradiated samples.

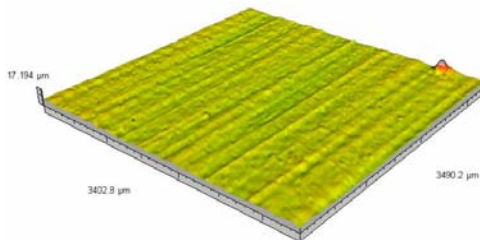


Figure 7 – Continuous axonometric for  $\text{CO}_2$  laser irradiated nylon 6,6 at  $5\text{W}$ ,  $1000\text{mms}^{-1}$  (Sample C10).

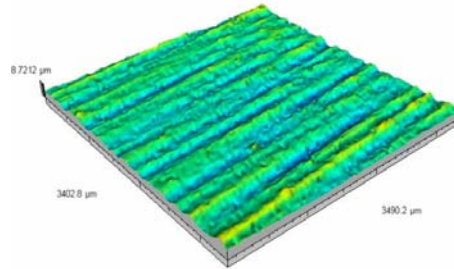


Figure 8 – Continuous axonometric for  $\text{CO}_2$  laser irradiated nylon 6,6 at  $8\text{W}$ ,  $1000\text{mms}^{-1}$  (Sample C9).

The surface roughness parameter Sa was determined for each of the surfaces. The Sa roughness value for the  $5\text{W}$   $\text{CO}_2$  laser irradiated nylon surface was  $0.262\mu\text{m}$ , whereas the higher power of  $8\text{W}$  gave rise to a slightly rougher surface with an Sa value of  $0.358\mu\text{m}$ . In addition, the effect the beam has had on the surface topography can be seen more prominently in Figures 7 and 8. However, by taking a profile extraction (Figures 9 and 10) of the surfaces perpendicular to the direction of the grooves, it can be seen that there was no fixed periodicity to the surface pattern. This is due to the fact that the spot size was larger than the intended surface pattern and the irradiation lines overlap.

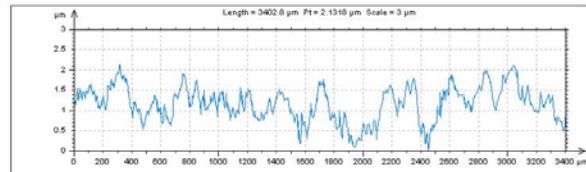


Figure 9 – Profile extraction of the surface shown in Figure 7, perpendicular to the grooves.

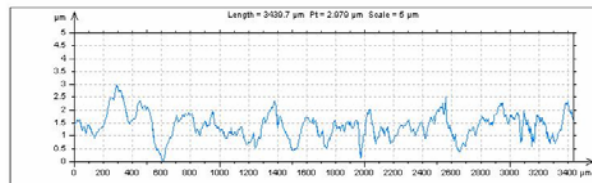


Figure 10 – Profile extraction of the surface shown in Figure 8, perpendicular to the grooves.

Figures 9 and 10 show that the maximum peak height observed for  $5\text{W}$  and  $8\text{W}$  laser powers were  $2$  and  $3\mu\text{m}$  respectively. Even though there was no fixed periodicity for the irradiated samples shown in Figures 9 and 10, it can be seen that there were distinct grooves produced in the nylon 6,6 as a result of the  $\text{CO}_2$  laser processing. This is more discernible when comparing the continuous axonometric images shown in Figures 7 and 8 with that of the non-irradiated reference sample

shown in Figure 5, along with the relative profile extraction curves.

Figures 11 and 12 show the continuous axonometric images for the F<sub>2</sub> excimer laser irradiated nylon surfaces for different pulse numbers per site.

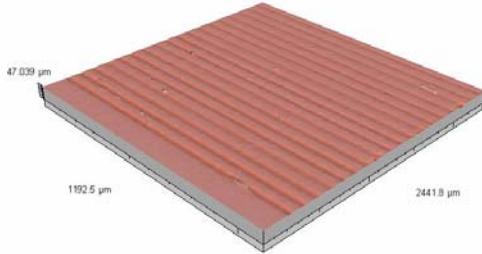


Figure 11 – Continuous axonometric image for F<sub>2</sub> excimer laser irradiated nylon 6,6 at 1,000 pulses per site (Sample F3).

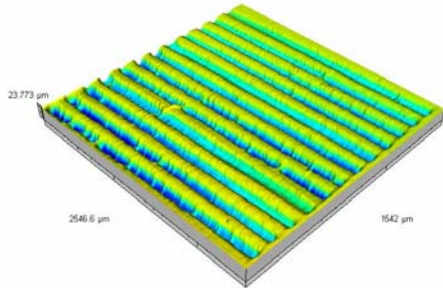


Figure 12 – Continuous axonometric image for F<sub>2</sub> excimer laser irradiated nylon 6,6 at 10,000 pulses per site (Sample F4).

The etched trenches using the F<sub>2</sub> excimer laser shown in Figures 11 and 12 were considerably more defined than the CO<sub>2</sub> laser irradiated samples (see Figures 7 and 8). In comparison to the CO<sub>2</sub> laser irradiated samples the pattern etched into the sample as shown in Figures 11 and 12 had a more distinct periodicity and can be easily identified with profile extractions as shown in Figures 13 and 14.

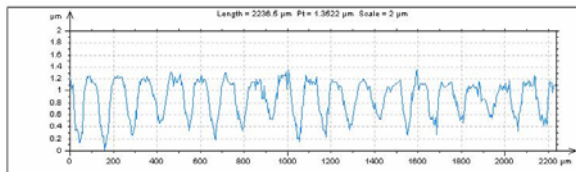


Figure 13 – Profile extraction of the surface shown in Figure 11, perpendicular to the grooves.

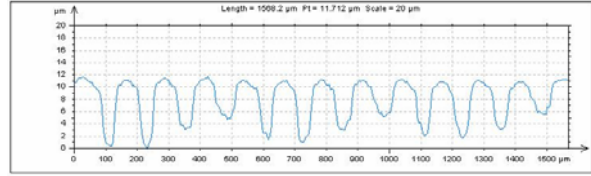


Figure 14 – Profile extraction of the surface shown in Figure 12, perpendicular to the grooves.

The roughness parameter, Sa, for the surface shown in Figure 11 was found to be 0.248μm, whereas the roughness for Figure 12 was found to be 2.647μm which was considerably greater than the other three samples due to the depth of the trenches being approximately 10μm. It should be noted that for the other three samples the surface features were around 2 to 5μm as can be seen in the other profile extractions (Figures 9, 10, 13 and 14). Using the non-irradiated sample as a reference it can be seen that both lasers are capable of increasing the roughness of the surface of nylon 6,6; however, as the F<sub>2</sub> excimer laser offers better precision and accuracy due to the etch rate for this particular system being of the order of 1nm per pulse it can be seen that the roughness can be more accurately controlled. This is contrasted with the CO<sub>2</sub> laser system as the surface pattern is dependant on the surface melting and resolidifying to produce a protrusion out of the surface which gives rise to a level of inaccuracy for the surface pattern.

#### Effects of Laser Irradiation on the Wettability Characteristics

As it has already been discussed, it is believed by many that the characteristic contact angle for a material is the potential driving force in regards to the prediction of how a biomaterial will perform within a biological environment. The dynamic advancing contact angles and hysteresis for triply distilled water for each of the samples can be seen in Table 1, along with the recorded three roughness parameters Sa, Ra and Wa for each sample.

Table 1 – A summary of the results for the seven samples along with their characteristic contact angle and hysteresis with triply distilled water.

Sample ID	Sa ( $\mu\text{m}$ )	Ra ( $\mu\text{m}$ )	Wa ( $\mu\text{m}$ )	Contact Angle ( $^{\circ}$ )	Hysteresis ( $^{\circ}$ )
CO <sub>2</sub> Laser Irradiated Samples					
C10	0.262	0.346	0.118	53.91	17.22
C9	0.358	0.256	0.190	52.36	19.82
F <sub>2</sub> Excimer Laser Irradiated Samples					
F3	0.248	0.253	0.021	66.67	31.05
F4	2.647	2.947	0.978	72.92	40.97
Emery Paper Roughened Samples					
R1	3.104	2.368	1.862	43.95	26.01
R2	3.735	3.055	3.568	38.37	22.25
Non-Irradiated Reference Sample					
N6	0.038	0.043	0.020	49.34	19.98

The surface roughness shown in Table 1, has been considerably increased, by up to an Ra of 2.904 $\mu\text{m}$ , in comparison to the non-irradiated sample using both laser systems. It can also be seen that the contact angle for each laser irradiated sample was increased with the F<sub>2</sub> excimer laser irradiated samples giving the largest change with a contact angle of 72.92 $^{\circ}$  for the roughest sample. This does not concur with current theory as the contact angle should decrease with increasing surface roughness [18,26]. Further studies of the surfaces were required in order to explain these results. The contact angles determined for the emery paper roughened surfaces were decreased in comparison to the non-irradiated sample and will be discussed in more detail later.

Using the SCA20 software the surface energy and components for each sample were obtained to try to explain the variation in contact angle and can be seen in Table 2.

Table 2 – Surface energies and components of each of the five samples.

Sample ID	Contact Angle ( $^{\circ}$ )	Polar Component ( $\text{mJm}^{-2}$ )	Dispersive Component ( $\text{mJm}^{-2}$ )	Total Surface Energy ( $\text{mJm}^{-2}$ )
CO <sub>2</sub> Laser Irradiated Samples				
C10	53.91	20.75	27.38	48.13
C9	52.36	24.27	23.90	48.17
F <sub>2</sub> Excimer Laser Irradiated Samples				
F3	66.67	9.78	37.19	46.98
F4	72.97	8.46	28.44	36.90
Emery Paper Roughened Samples				
R1	43.95	22.57	34.86	57.43
R2	38.37	24.68	36.85	61.53
Non-Irradiated Reference Sample				
N6	49.34	20.15	36.12	56.27

The data given in Table 2 shows significant changes within the surface energy components in comparison to the non-irradiated reference sample used. After CO<sub>2</sub> laser irradiation the total surface energy was slightly reduced due to a change in polar and dispersive components. It can be seen that the polar component increases by up to 4.12 $\text{mJm}^{-2}$  for the rougher sample, whereas the dispersive component was reduced by 12.22 $\text{mJm}^{-2}$ . As it is the polar component of the surface energy that plays the major role in determining the contact angle it can be seen that these results do not correspond with existing theory. For instance, Lawrence and Li [17] state that a laser-induced increase in the polar component, along with an increase in O<sub>2</sub> content, would give rise to a reduction in the contact angle.

Following on, subsequent to F<sub>2</sub> excimer laser irradiation the polar component of the surface energy was considerably reduced by up to 10 $\text{mJm}^{-2}$ . This substantial reduction in polar component could be seen to be the main reason as to why there is a significant increase in the contact angle. The dispersive component is quite inconclusive due to the fact that both results lay either side of the value determined for the reference sample. As a result of this, further research may be required to determine the trend of the dispersive component in this case and could be used as a further study to confirm the results achieved here. However, it still can be seen that the total surface energy determined for the F<sub>2</sub> excimer laser irradiated samples was somewhat lower with 36.9 $\text{mJm}^{-2}$  for sample F4.

In order to determine if these changes in surface energies were as a result of variations in surface chemistry three samples were chosen for XPS and EDX analysis. Table 3 shows the surface O<sub>2</sub> content for selected samples.

Table 3 – Surface O<sub>2</sub> content for selected samples

Sample ID	Surface O <sub>2</sub> Content (%)	Contact Angle ( $^{\circ}$ )
C10	22.23	53.91
F3	17.48	66.67
R1	20.70	43.95
N6	20.76	49.34

The non-irradiated reference sample showed that, in terms of weight, 79.24% was carbon and 20.76% was oxygen. In comparison with the CO<sub>2</sub> laser irradiated sample the oxygen content had risen slightly to 22.23%, whereas the F<sub>2</sub> excimer laser irradiated sample was found to have less oxygen content with only 17.48%. The oxygen in the ambient air of the CO<sub>2</sub> system could have possibly allowed oxidation of the surface to occur as the molten nylon re-solidified.

Additionally, as the  $F_2$  excimer laser system was under vacuum, there would have been a reduction in oxygen and as a result the surface would not oxidize and could potentially lose oxygen content during the laser ablation process.

Due to the ability of using these laser systems to manipulate the wettability characteristics further research can also be made by carrying out biological testing of the laser irradiated samples. This would determine if cell adhesion and proliferation can be optimized by using these lasers to produce surface modification in terms of surface chemistry and surface topography. In addition, as nylon 6,6 has a high water absorption rate it may be possible to identify, through extended research, whether surface modifications using laser technology allows this parameter to be reduced. By experimenting with different ambient gases it may also be possible to inflict greater chemical changes on the surface of the material allowing for further studies of how the chemical nature of the surface gives rise to the variation in contact angle and surface energy.

#### Determination of Active Wetting Regime

As it has already been shown, surface energy, XPS and EDX analysis for the  $CO_2$  laser irradiated samples should allow the samples to have a contact angle that is lower than the contact angle determined for the non-irradiated sample. To clarify this, two samples were roughened using emery paper, of which the continuous axonometric images can be seen in Figure 15 and 16, in order to find some explanation for this phenomenon.

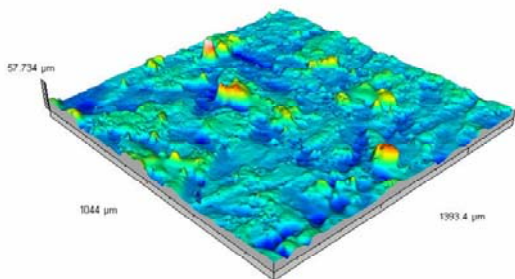


Figure 15 – Continuous axonometric image of the first emery paper roughened sample (Sample R1).

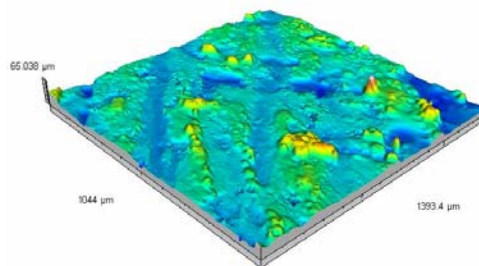


Figure 16 – Continuous axonometric image of the second emery paper roughened sample (Sample R2).

As a result of the mechanical roughening of the samples it can be seen in Tables 1 and 2 that an increase in polar component and roughness has given rise to a significant reduction in contact angle, which agrees with Lawrence and Li [17]. It must be stated at this point that the images shown in Figures 15 and 16 give an indication that no periodic pattern had been induced on the surface of the nylon 6,6 samples. In contrast, the laser irradiated samples have more periodic patterns relative to the manually roughened surfaces. These periodic patterns appear to have an extremely large affect on the wettability of the samples. As discussed by Jung and Bhushan [27] there are two regimes in which a material can wet; these being the Cassie-Baxter and Wenzel regimes. In which the Wenzel regime, shown in Figure 17, allows the whole sample to be wetted such that the droplet is in complete contact with the surface.



Figure 17 – Schematic diagram showing a droplet of water on a patterned surface giving rise to the Wenzel wetting regime.

On the other hand, the Cassie-Baxter regime, shown in Figure 18, allows the droplet to rest upon the roughened surface peaks forming air gaps between the droplet and the surface.

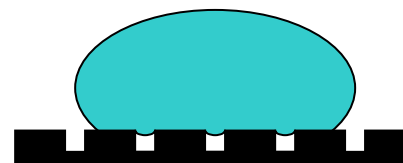


Figure 18 – Schematic diagram showing a droplet of water on a patterned surface giving rise to the Cassie-Baxter wetting regime.

It is proposed here that a change from the Wenzel regime to the Cassie-Baxter regime was the likely



reason for the observed increase in the contact angle for the CO<sub>2</sub> laser irradiated samples and the F<sub>2</sub> excimer laser irradiated samples. This would be due to the fact that the Cassie-Baxter regime inherently gives rise to larger contact angles in comparison to the Wenzel regime. Therefore, it is also proposed that the surface pattern is the main driver for the manipulation of the wettability characteristics, implying that the surface roughness (Table 1), surface energy components (Table 2) and surface O<sub>2</sub> content (Table 3) do not play a governing role. In order to confirm this proposal more research into which wetting regime takes place is required.

### Conclusions

It has been demonstrated that both the CO<sub>2</sub> and F<sub>2</sub> excimer laser systems that have been employed in this study have the ability to modify the surface of nylon 6,6. The CO<sub>2</sub> laser couples into the material via resonant coupling which gives rise to bond vibrations allowing the temperature to rise and melt the material. Upon cooling the molten material re-solidifies and a protrusion away from the surface becomes evident on the surface. This is contrasted with the F<sub>2</sub> excimer laser as it ablates the nylon 6,6 allowing the required pattern to be etched into the material. As a result the F<sub>2</sub> excimer laser system offers a major advantage over the CO<sub>2</sub> in the fact that it ablates approximately 1nm per pulse, with the fluence used in this instance, allowing the user to be precise and accurate with the surface topography they require. However, the amount of time it takes to pump the F<sub>2</sub> vacuum system to operating pressure and the amount of time it takes to produce a number of few µm deep trenches is considerably greater than the CO<sub>2</sub> laser system employed in this study.

Both of the laser systems affect differently the nylon 6,6 samples with regards to wettability and surface energy parameters – two major factors which are believed to manipulate the bioactivity of a material in regards to cell adhesion and proliferation. The CO<sub>2</sub> laser has been seen to be capable of producing contact angles slightly larger in comparison to an unirradiated reference sample. This does not agree with current theory as the increased polar component and increased O<sub>2</sub> content should give rise to a reduction in contact angle. For instance the F<sub>2</sub> excimer laser irradiated samples gave larger contact angles which seems to be the result of a decrease in polar component and decrease in O<sub>2</sub> content. However, it has been proposed here that the increases in the contact angle for both laser systems could also be due to the fact that the sample surfaces are patterned, such that they give rise to a change in wetting regime from Wenzel type to the

Cassie-Baxter regime. This may allow one to see how the CO<sub>2</sub> laser irradiated samples would give a larger contact angle in comparison to the non-irradiated sample. This would imply that the surface pattern dominates the wettability characteristics of the material. In order to confirm this proposal much more research is required into how the droplet forms on the sample surface.

### Acknowledgements

We would like to thank Matthew Gibson, Peter Wileman and David Britton for all of their much appreciated support. This study is financially supported by the EPSRC (No. EP/E046851/1).

### References

1. Mao, C. et al. (2005) In vitro studies of platelet adhesion on UV radiation-treated nylon surface. *Carbohydrate Polymers*, 59, 19-25.
2. Karaca, E. et al. (2008) Analysis of the Fracture Morphology of Polyamide, Polyester, Polypropylene, and Silk Sutures Before and After Implantation In Vivo. *Journal of Biomedical Materials Research Part B: Applied Biomaterials*.
3. Makropoulou, M. et al. (1995) Ultra-violet and Infra-red Laser Ablation Studies of Biocompatible Polymers. *Lasers in Medical Science*, 10, 201-206.
4. Benson, R. S. (2002) Use of Radiation in Biomaterials Science. *Nuclear Instruments and Methods in Physics Research B*, 191, 752-757.
5. Arefi-Khonsari, F. et al. (2005) Processing of Polymers by Plasma Technologies. *Surface and Coatings Technology*, 200, 14-20.
6. Pappas, D. et al. (2006) Surface Modification of Polyamide Fibers and Films using Atmospheric Plasmas. *Surface and Coatings Technology*, 201, 4384-4388.
7. Harnett, E. M. et al. (2007) The surface energy of various biomaterials coated with adhesion molecules used in cell culture. *Colloids and Surfaces B: Biointerfaces*, 55, 90-97.
8. Yu, F. et al. (2005) Laser interference lithography as a new and efficient technique for micropatterning of biopolymer surface. *Biomaterials*, 26, 2307-2312.
9. Mirzadeh, H. et al. (2003) Influence of laser surface modifying of polyethylene terephthalate on fibroblast cell adhesion. *Radiation Physics and Chemistry*, 67, 381-385.

10. Silfvast, W. T. (1996) *Laser fundamentals*. Cambridge, UK. Cambridge University Press.
11. Skordoulis, C. D. et al. (1995) Ablation of nylon-6,6 with UV and IR lasers. *Applied Surface Science*, 86, 239-244.
12. Duncan, A. C. et al. (2002) Laser Microfabricated Model Surfaces for Controlled Cell Growth. *Biosensors & Bioelectronics*, 17, 413-426.
13. Pflöging, W. et al. (2007) Laser-Assisted Modification of Polystyrene Surfaces for Cell Culture Applications. *Applied Surface Science*, 253, 9177-9184.
14. Callewaert, K. et al. (2003) Excimer Laser Induced Patterning of Polymeric Surfaces. *Applied Surface Science*, 208-209, 218-225.
15. Tiaw, K. S. et al. (2007) Precision Laser Micro-Processing of Polymers. *Journal of Alloys and Compounds*.
16. Sarantopoulou, E. et al. (2007) Polymer Self-Assembled Nano-Structures and Surface Relief Gratings Induced with Laser at 157nm. *Applied Surface Science*, 253, 7884-7889.
17. Lawrence, J. et al. (2001) Modification of the Wettability Characteristics of Polymethyl Methacrylate (PMMA) by Means of CO<sub>2</sub>, Nd:YAG, Excimer and High Power Diode Laser Irradiation. *Materials Science and Engineering A*, 303, 142-149.
18. Hao, L. et al. (2005) *Laser surface treatment of bio-implant materials*. New Jersey, USA: John Wiley & Sons Inc.
19. Lai, J. et al. (2006) Study on Hydrophilicity of Polymer Surfaces Improved by Plasma Treatment. *Applied Surface Science*, 252, 3375-3379.
20. Ma, Z. et al. (2007) Surface modification and property analysis of biomedical polymers used for tissue engineering. *Colloids and Surfaces B: Biointerfaces*, 60, 137-157.
21. Vogler, E. A. (2004) Role of water in biomaterials. In: Ratner, B. D. et al., editor. *Biomaterials Science*. Second ed. San Diego, California, USA. Elsevier Academic Press.
22. Van, O. et al. (1975) *Phagocytic engulfment and cell adhesiveness*. New York, USA. Marcel Dekker.
23. Kim, M. S. et al. (2007) Gradient polymer surfaces for biomedical applications. *Progress in Polymer Science*.
24. Ball, M. D. et al. (2004) Cell interactions with laser-modified polymer surfaces. *Journal of Materials Science: Materials in Medicine*, 15, 447-449.
25. Rance, D. G. (1982) Chapter 6 - thermodynamics of wetting: From its molecular basis to technological application. In: Brewis, D. M. (editor). *Surface Analysis and Pretreatment of Plastics and Metals* Essex, UK. Applied Science Publishers.
26. Lawrence, J. et al. (2001) *Laser modification of the wettability characteristics of engineering materials*. Suffolk, UK. Professional Engineering Publishing Limited.
27. Jung, Y. C. et al. (2007) Wetting transition of water droplets on superhydrophobic patterned surfaces. *Scripta Materialia*, 57, 1057-1060.

### **Meet The Author**

David Waugh is currently undertaking a Ph.D at the Wolfson School of Mechanical and Manufacturing Engineering, Loughborough University, UK under the supervision of Dr. Jonathan Lawrence. His research is focusing on using laser surface treatment of polymeric biomaterials for enhanced cell response. He obtained his MPhys Hons. in Physics with Lasers and Photonics and MSc in Laser Applications in Micro-Machining and Processing from the University of Hull, UK.